

RIIM ACCELERATOR BEAM EXPERIMENTS

M. G. Mazarakis, D. L. Smith, R. B. Miller, R. S. Clark, D. E. Hasti,
D. L. Johnson, J. W. Poukey, K. R. Prestwich, and S. L. Shope

Sandia National Laboratories
Albuquerque, New Mexico 87185

and

R. D. Richardson

Science Applications International Corporation
Albuquerque, New Mexico 87109

Abstract

A pulsed linear accelerator assembly, RIIM (RADLAC II Module), composed of an injector plus a number of post accelerating gaps was built and successfully operated. The injector and the post accelerating gaps were powered by water strip pulse forming and transmission lines. A high-current, high-voltage, foilless diode injector was used and an annular 40-kA relativistic electron beam was produced and further accelerated through the post accelerating gaps. The final beam energy was close to the sum of injector and gap voltages and equal to 9 MeV.

Introduction

We are exploring high current (25-80 kA) linear induction electron accelerator concepts. RADLAC I, a 9-MV, 25-kA, radial transmission line accelerator, and MABE, a 7-MeV, 80-kA accelerator development facility, have been described in previous publications. [1,2] In this paper, we describe the design and performance of the RADLAC-II Module (RIIM), a concept that extends technology to increase the accelerating voltage per gap and improves our knowledge of high current beam transport issues. RIIM is designed to provide unrestricted access to the beam line. Achieving this access was accomplished by powering the beam line by water-dielectric strip transmission lines based on PBFA I [3] instead of the completely closed cavity construction of RADLAC I. This open construction is less efficient in coupling energy to the accelerating gap than RADLAC I. Stripline geometries have been investigated to optimize the energy transfer efficiency and are described briefly in third section of this paper. A 9-MeV, 40-kA electron beam has been generated by the injector and two accelerating gaps in RIIM.

Accelerator Description

The accelerator is composed of a Marx generator, an intermediate storage capacitor (ISC), pulse forming transmission lines (PFL), transmission line convolutes, and the beam line. The 4-MV Marx generator with 40, 1.3- μ F, 100-kV capacitors is the primary energy source. The Marx generator charges a coaxial/water-dielectric ISC through a coaxial oil transmission line and oil/water interface. The ISC has the same capacitance as the Marx generator and reaches peak voltage in about 1.2 μ s. The PFL and transmission lines are tri-plate water-dielectric lines which are charged when two laser-triggered spark gaps close, transferring the energy from the ISC to the PFLs. A frequency quadrupled ND:YAG laser focused between the switch electrodes trigger the gas switches with 1- σ jitter less than 2.3 ns. [4] The rapid charging of the PFL (~ 250 ns) permits the use of

self-closing, water-dielectric switches which deliver a 50-ns pulse to a split diamond-shaped convolute as shown in Fig. 1. One of the convolute legs inverts the pulse polarity, via crossover bars, so that the voltage applied on the diode would be ideally twice the transmission line voltage. The diamond-shaped convolute region is necessary to avoid short-circuiting the inverter during the pulse. It appears as a shunt impedance to the transmission line, and the actual convolute voltage gain is 1.8. Each diode is powered by two PFLs and transmission lines located above and below the beam line axis. The lines make a 90° turn and feed the diode from two opposite sides to assure diode magnetic field uniformity to prevent beam steering. The injector is powered by four PFLs providing twice the post-accelerating gap voltage to a foilless diode electron source (Fig. 2).

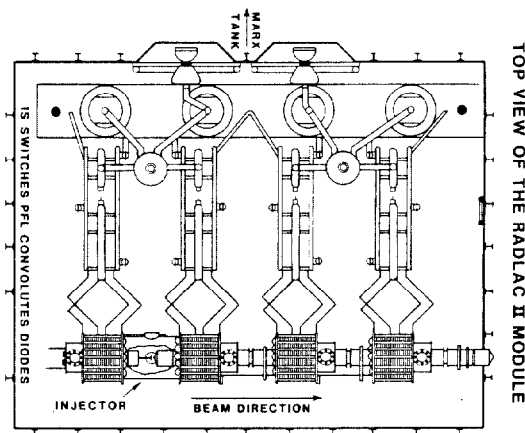


Figure 1: Top view of RADLAC II Module with the convolutes modified to increase transmission efficiency by 40%.

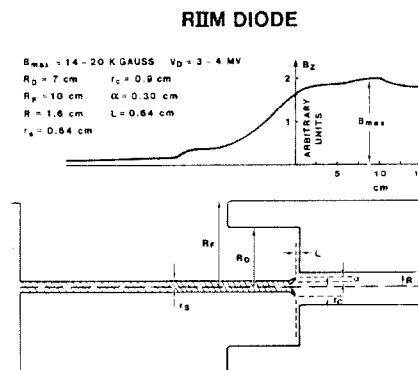


Figure 2: RIIM foilless diode design parameters.

Beam Line Power Flow Considerations

Since the beam line is not fully enclosed by an accelerating cavity, the accelerating gaps must be separated by the distance that an electromagnetic wave would travel during the accelerating pulse so that voltage with respect to ground along the beam line never exceeds the output voltage of each transmission line. The open construction also allows electromagnetic waves to propagate into the surrounding water, thereby charging stray capacitances. This charging represents an energy loss during the accelerating pulse. In the initial design, the $20\ \Omega$ transmission lines feeding the accelerating gaps had an aspect ratio (width/gap spacing) approximately equal to one. With this aspect ratio, the energy required to charge the stray capacitances reduced the accelerating voltage substantially below the values originally estimated from modeling studies. The convolutes and transmission lines were reconfigured as shown in Fig. 3 to improve the aspect ratio. This modification resulted in a 40% increase in the accelerating voltage.

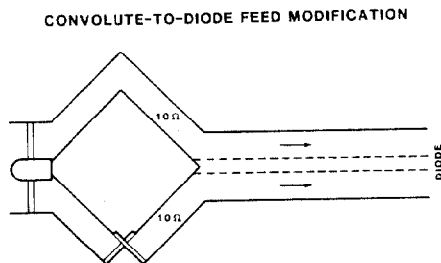


Figure 3: Convolute-to-diode feed modification. The solid lines represent the original design. The broken lines represent the present configuration also shown in Fig. 1.

Beam Generation and Acceleration

The four PFLs that power the injector provide greater than ~ 4 MV to a foilless diode electron source. The foilless diode generates a thin, hollow, high current beam which is necessary to overcome space charge effects in the low voltage end of the accelerator. The electron beam is borne in the solenoidal magnetic field which is used to transport the beam through the accelerator.

A schematic diagram of the foilless diode is shown in Fig. 2 together with the relevant dimensions. The design goals were 40–60 kA at a 4 MV diode voltage. The anode cathode gap can be varied continuously from the outside without breaking the accelerator beam line vacuum. The annular beam is guided through the accelerator by a 17–20 kG axial magnetic field. The field is provided by an array of solenoidal coils connected to a number of capacitor banks. An improved accelerating gap design [5] maintains radial force balance and completely eliminates the previously observed (RADLAC I) [1] beam radial oscillations. In addition, the accelerating cavities ("diodes") of the injector and post accelerating gaps have a very low Q and very small transverse shunt impedance Z_{\perp} eliminating the growth of the beam break-up instability. [5] The application of the peak voltage to the diodes is synchronized to coincide with the arrival of the beam pulse in each gap. This is accomplished by adjusting the laser path length to fire the spark gaps in the correct time sequence.

The beam current was measured by three Rogowski coils. One was located between the injector and the first post accelerating gap and the other two were downstream from the first and second gaps (Fig. 1). The injector and post accelerating gap voltage were measured by resistive monitors. Samples of diode voltage waveforms are presented in Fig. 4. An experimental injector parameter optimization study combined with numerical simulations led to a beam current in the order of 40 kA (Fig. 5). Figure 5 also shows the achieved effective accelerating voltage throughout the entire machine. Because of excellent switch synchronization, the total effective accelerating voltage is close to the sum of diode voltages. Effective accelerating voltage is the sum of all the diode voltages as measured by the resistive

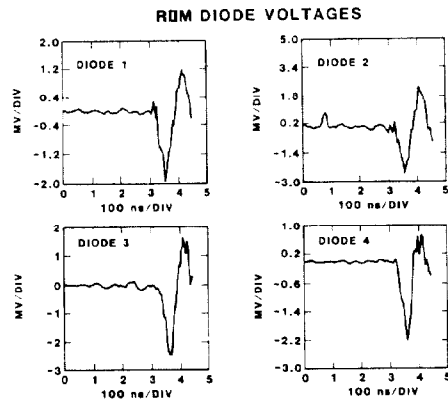


Figure 4: Sample of diode voltage waveforms for 85 kV, Marx charging. Diode voltages 1 and 2 add across the injector.

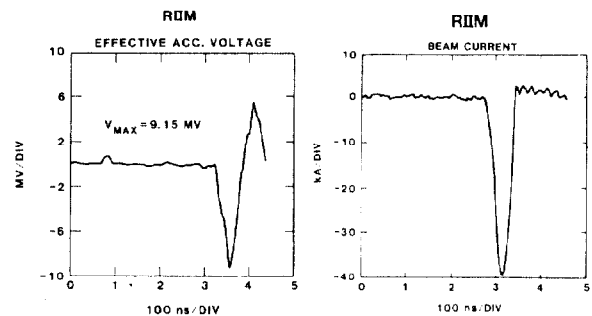


Figure 5: Beam current and effective accelerating voltage throughout the entire machine.

monitors corrected for timing. The beam profile and cross section was observed in many locations along its path. Brass witness plates and radiochromic foils were used. Because of the high power density of the beam annulus, it was difficult to precisely measure beam size on brass targets. Figure 6 gives beam damage patterns obtained immediately downstream from the injector and at the end of the accelerator.

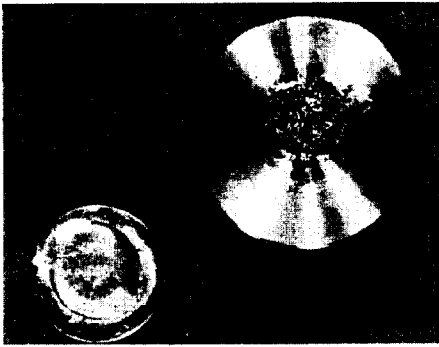


Figure 6: Beam pattern profile on brass targets. The left target was placed immediately downstream from the injector. The right one was at the end of the accelerator.

References

- [1] R. B. Miller, et. al., J. Appl. Phys. 52, 1184
- [2] K. R. Prestwich, et. al., IEEE Trans. Nucl. Sci. 30, No. 4, 3155, 1983
- [3] J. P. VanDevender, "Pulsed Power Fusion Systems for Inertial Confinement Fusion." National Electronics Conference, Energy Research Session, Oct. 1979, Chicago, IL
- [4] R. A. Hamil, et. al., IEEE Proceedings of the 4th Internat'l Pulsed Power Conference, Albuquerque, NM, June 1983, p. 447.
- [5] M. G. Mazarakis, et. al., Proceedings of the 1984 Linear Accelerator Conference, Darmstadt (1984), GSI-84-11, p. 466

Table I summarizes the RIIM performance for two Marx charging voltages.

Table I
Summary of RIIM Performance

| Marx Charging Voltage (kV) | Average Gap Voltage (MV) | Sum of Gap Voltages (MV) | Effective Acc. Voltage (MV) | Beam Current (kA) |
|----------------------------|--------------------------|--------------------------|-----------------------------|-------------------|
| 75 | 2.06 | 8.25 | 7.30 | 20 |
| 85 | 2.34 | 9.35 | 9.06 | 40 |

Conclusion

A reliable, high-current linear induction accelerator, RIIM, has been developed. The modifications to the transmission lines have improved the overall power flow, resulting in a 40% improvement in the accelerating voltage per gap. The accelerating voltage met the original design goals. The final energy, 9 MeV, is close to the sum of the injector and post-accelerating gap voltages (9.35 MV). The optimized injector and accelerating gaps have produced a 40-kA, 9-MeV, annular electron beam.

Acknowledgments

This work was supported by the U. S. Department of Energy under Contract #DE-AC04-76-DP00789 and by the Air Force Weapons Laboratory. The authors would like to thank G. Denison, D. Hendricks, E. Jones, and J. Bazar for their hard and innovative work in building RIIM and their valuable assistance with the first stage of performance tests; the RIIM operations team, D. Armistead, D. Bolton, T. Coffman, and W. Olson for implementing the machine modifications, assisting with the data analysis, and for the many hardware improvement ideas; and L. Stevenson for his most valuable assistance in setting the data collection computer system and diagnostic calibration. Finally, the support, patience, and encouragement of G. Yonas, D. Straw, J. Head, and W. Baker is also gratefully acknowledged.